

Supramolecular Assembly and Ab Initio Quantum Chemical Calculations of 2-Hydroxyethylammonium Salts of *para*-Substituted Benzoic Acids

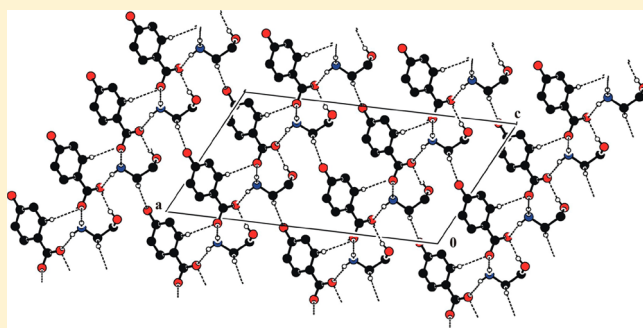
Manuela Crisan,[†] Paulina Bourosh,[‡] Yuri Chumakov,^{*,‡} Mihaela Petric,[†] and Gheorghe Ilia[†]

[†]Institute of Chemistry Timisoara of Romanian Academy, 24 Mihai Viteazul Boulevard, Timisoara, 300223, Romania

[‡]Institute of Applied Physics, Academy of Sciences of Moldova, Academiei Street 5, Chisinau, MD - 2028, Republic of Moldova

Supporting Information

ABSTRACT: Crystal structures of seven salts of 2-hydroxyethylamine with benzoic acid (1) and different substituted benzoic acids, such as *p*-methylbenzoic acid (2), *p*-methoxybenzoic acid (3), *p*-hydroxybenzoic acid (4), *p*-chlorobenzoic acid (5), *p*-bromobenzoic (6), and *p*-iodobenzoic (7) have been studied. The salts units of 1–7 serve as building blocks (BB) of the supramolecular architecture. In a crystal they are held together *via* proton-transferred N–H···O and normal O–H···O hydrogen bonds. The substituents on anions influence dipole–dipole interactions between anions and cations in molecular aggregates. As a result, they are organized in building blocks either *via* one charge-assisted (1, 2) hydrogen bond or *via* two (3–7) hydrogen bonds. The dispersion interaction significantly contributes to intermolecular force fields driving the organization of hydrogen bonds in BB. In all studied compounds, building blocks are consolidated into 2-D layers through the N–H···O and O–H···O hydrogen bonds. For the crystal structures of 2–7, with non-centrosymmetric space groups and the BB self-assembled by two hydrogen bonds, the macroscopic polarizations of a unit cell is practically perpendicular to the layers.



INTRODUCTION

In recent years, there has been considerable interest in the synthesis and complex study of multicomponent organic crystals built from acid–base complexes. Multicomponent crystals, e.g., solvates, hydrates, co-crystals, and salts, play an important role in the predictable assembly of supramolecular architectures, host–guest materials, interpenetrated networks, solid-state reactivity, topochemical reactions, pharmaceutical co-crystals, and polymorphism.¹ Supramolecular architectures based on noncovalent interactions are fascinating and have attracted a great deal of attention. Central in the present study of intermolecular interactions is the hydrogen bond, which is the most energetic and directional bond.² Weak interactions, such as C–H···O, C–H···N, C–H···X (X = Cl, Br, I), are of considerable significance (in the absence of classical hydrogen bonds) because they play an important role in the molecular packing arrangement. Therefore, an important application is the use of self-assembly of small molecules with hydrogen bonds and other weaker intermolecular interactions in creation of one-, two-, and three-dimensional networks.³ This is why organic salts⁴ have been increasingly studied in crystal engineering, other motives being their better predictability due to robust charge-assisted hydrogen-bonded supramolecular synthons and their greater thermal stability compared to that of their neutral counterparts.⁵ Organic salts have some advantages over neutral organic molecules:⁶ hydrogen bonds between ions

are generally stronger than those between neutral molecules, and the ability of cations and anions to function as hydrogen-bonding donors or acceptors can be tuned using acid–base chemistry. Therefore, in the present study, we investigate the molecular packing in crystalline materials using organic salts as molecular building blocks. Aromatic carboxylic acids have attracted our interest because of their importance in crystal engineering and their ability to form strong and directional hydrogen bonds.⁷ Many carboxylic acids are widely used in pharmaceutical salts and co-crystals. For example, benzoic acids, in spite of their simple structure, present complex effects as pharmacological, plant growth regulators, antibacterial and antifungal agents.⁸ It is also known that 2-hydroxyethylamine is a good organic base and has hydrogen-bond donor sites. On the other hand, 2-hydroxyethylamine (ethanolamine) is an essential component of cell membranes, closely resembling that of choline chemical behavior. Some complexes of ethanolamine with organic and inorganic compounds appear to be promising for optical second harmonic generation and electrooptical properties.⁹ Therefore, preparation of multicomponent organic crystals from such multifunctional molecules as aromatic carboxylic acids and 2-hydroxyethylamine is expected to display

Received: September 7, 2012

Revised: November 21, 2012

Table 1. Crystal Data and Structure Refinement Parameters for 1–7

compounds	1	2	3	4	5	6	7
formula	C ₉ H ₁₃ N ₁ O ₃	C ₁₀ H ₁₅ N ₁ O ₃	C ₁₀ H ₁₅ NO ₄	C ₉ H ₁₃ N ₁ O ₄	C ₉ H ₁₂ Cl ₁ N ₁ O ₃	C ₉ H ₁₂ Br ₁ N ₁ O ₃	C ₉ H ₁₂ I ₁ N ₁ O ₃
fw	183.20	197.23	213.23	199.20	217.65	262.11	309.10
wavelength	0.71073	1.54184	0.71073	1.54184	0.71073	1.54184	0.71073
crystal system	orthorhombic	orthorhombic	orthorhombic	monoclinic	orthorhombic	orthorhombic	orthorhombic
space group	<i>Pbca</i>	<i>Iba2</i>	<i>P2₁-2₁-2₁</i>	<i>Cc</i>	<i>Pna2₁</i>	<i>Pna2₁</i>	<i>Pna2₁</i>
<i>a</i> , Å	7.909(2)	9.795(2)	6.189(1)	21.318(4)	6.026(1)	6.029(1)	6.029(1)
<i>b</i> , Å	11.011(2)	26.905(5)	14.891(3)	4.4990(9)	7.384(2)	7.352(2)	7.352(2)
<i>c</i> , Å	21.752(4)	7.9890(16)	23.594(5)	11.179(2)	23.049(5)	23.192(5)	23.192(5)
α , deg	90	90	90	90	90	90	90
β , deg	90	90	90	116.69(3)	90	90	90
γ , deg	90	90	90	90	90	90	90
<i>V</i> , Å ³	1894.1(7)	2105.4(7)	2174.4(7)	957.9(3)	1025.4(4)	1028.0(4)	1028.0(4)
<i>Z</i>	8	8	8	4	4	4	4
ρ_{calc} mg/m ³	1.285	1.244	1.303	1.381	1.410	1.694	1.997
μ , mm ⁻¹	0.097	0.758	0.101	0.921	0.353	5.332	3.097
<i>F</i> (000)	784	848	912	424	456	528	600
dimensions, (mm)	0.25 × 0.15 × 0.1	0.22 × 0.14 × 0.08	0.16 × 0.12 × 0.1	0.18 × 0.14 × 0.09	0.2 × 0.15 × 0.1	0.15 × 0.15 × 0.1	0.2 × 0.2 × 0.1
θ range for data collection, deg	1.87–25.99	3.29–69.97	1.62–25.50	4.64–70.00	1.77–25.49	3.81–69.99	1.76–25.00
index ranges	$-9 \leq h \leq 9, -13 \leq k \leq 13, -26 \leq l \leq 26$	$-11 \leq h \leq 11, -32 \leq k \leq 15, -9 \leq l \leq 3$	$-7 \leq h \leq 7, -18 \leq k \leq 16, -28 \leq l \leq 28$	$25 \leq h \leq 15, -5 \leq k \leq 5, -13 \leq l \leq 13$	$-7 \leq h \leq 7, -8 \leq k \leq 8, -27 \leq l \leq 27$	$-7 \leq h \leq 1, -8 \leq k \leq 8, -27 \leq l \leq 28$	$0 \leq h \leq 7, 0 \leq k \leq 8, 0 \leq l \leq 27$
reflections collected/unique	15973/1860	1077/1077	14974/3991	954/915	8955/1905	1006/1006	925/925
completeness (%)	$R(\text{int}) = 0.0272$ 99.9($\theta = 25.99$)	$R(\text{int}) = 0.000$ 100($\theta = 69.97$)	$R(\text{int}) = 0.0568$ 98.9($\theta = 25.50$)	$R(\text{int}) = 0.0181$ 100.0($\theta = 70.00$)	$R(\text{int}) = 0.0361$ 100.0($\theta = 25.49$)	$R(\text{int}) = 0.0000$ 100($\theta = 69.99$)	$R(\text{int}) = 0.0000$ 99.6($\theta = 25.00$)
data/parameters	1860/119	1077/129	3991/274	915/132	1905/129	1006/128	925/128
GOF on <i>F</i> ²	1.012	1.008	1.006	1.037	1.017	1.003	1.019
final <i>R</i> indices ($>2\sigma(I)$)	$R_1 = 0.0340, wR_2 = 0.0900$	$R_1 = 0.0375, wR_2 = 0.1027$	$R_1 = 0.0474, wR_2 = 0.1272$	$R_1 = 0.0286, wR_2 = 0.0831$	$R_1 = 0.0258, wR_2 = 0.0556$	$R_1 = 0.0183, wR_2 = 0.0543$	$R_1 = 0.0494, wR_2 = 0.1252$
<i>R</i> indices (all data)	$R_1 = 0.0459, wR_3 = 0.0958$	$R_1 = 0.0499, wR_2 = 0.1091$	$R_1 = 0.0665, wR_2 = 0.1355$	$R_1 = 0.0290, wR_3 = 0.0836$	$R_1 = 0.0319, wR_3 = 0.0572$	$R_1 = 0.0185, wR_2 = 0.0545$	$R_1 = 0.0497, wR_2 = 0.1255$
largest diff peak and hole, e ⁻ Å ⁻³	0.163/−0.193	0.149/−0.140	0.352/−0.187	0.129/−0.144	0.134/−0.117	0.280/−0.246	2.647/−2.285

interesting networks and useful properties. With this background, a class of salts formed by 2-hydroxyethylamine with aromatic carboxylic acids was prepared to investigate their supramolecular synthons. In our previous work,⁶ we have investigated the crystal structures of some organic salts containing the same anion *p*-nitrobenzoic acid and different cations, such as amino alcohols and morpholine. A structural study revealed that those compounds form supramolecular systems with different topologies on the basis of hydrogen bonding arrays as a function of properties of the donor and acceptor parts of the molecules. The objective in the present investigation is to extend the previous work on the molecular packing in the crystal structures of the seven 2-hydroxyethylammonium salts of *p*-substituted benzoic acids having the same cation. One component has a carboxyl group as an electron donor, and the other has an amino group or a nitrogen atom as an electron acceptor. Benzoic acids have been widely employed in constructing supramolecular architectures mainly in combination with organic bases, such as piperazine,¹⁰ imidazole,¹¹ benzylamine,¹² morpholinium,¹³ and quinoline.¹⁴ The complex formation of these compounds takes place only *via* proton transfer from the carboxyl group of an organic acid to the amino group or the nitrogen atom from the second component. In contrast, only a few examples of crystals of substituted benzoic acids with 2-hydroxyethylamine (ethanolamine) have been reported,¹⁵ including our crystals reported earlier.⁶ Therefore, the searching through the Cambridge Structural Database^{16,17} (version 5.33) has been performed in order to find all salts with *p*-substituted benzoic acids having the proton-transferred hydrogen bonds $\text{NH}^+\cdots\text{O}^-$ less than 2.2 Å. The total number of the found structures is 356. Among these compounds we have observed 52, 25, 11, 4, 11, 6, 1 hits for *p*-R substituted benzoic acids, where R=H, OH, CH₃, OCH₃, Cl, Br, I, respectively, but for the above-mentioned substituents no compounds having the same cation have been noticed. For of *p*-H, -OH, -CH₃, -OCH₃ substituents we found 9, 6, 3, 1 hits, respectively, where salts generate the supramolecular synthons with different dimensions in which the cations and anions are held together by two $\text{NH}^+\cdots\text{O}1^-$ and $\text{XH}\cdots\text{O}2$ hydrogen bonds *via* carboxylic group. In these synthons, the cations are bulky and can be divided into two groups: one group containing the fragment $-\text{OH}-(\text{CH}_2)_n-\text{N}^+\text{H}_2-$, ($n = 1, 2$) and the other the fragment $\text{NH}_2-\text{C}(=\text{R})-\text{N}^+\text{H}=\text{}$, ($\text{R}=\text{C}, \text{N}$), where the protonated subfragment without NH_2 -group belongs to the aromatic ring.

In the present paper, we report the synthesis, crystallographic studies, and *ab initio* quantum calculations of 2-hydroxyethylamine with benzoic acid (1) and different substituted benzoic acids, such as *p*-methylbenzoic acid (2), *p*-methoxybenzoic acid (3), *p*-hydroxybenzoic acid (4), *p*-chlorobenzoic acid (5), *p*-bromobenzoic (6), and *p*-iodobenzoic (7). Our previous studies reported biological activity and low-toxicity of these compounds.^{18–20} Single-crystal X-ray diffraction experiments have been carried out for all of the investigated salts in order to analyze their supramolecular architectures.

EXPERIMENTAL SECTION

General. All the reagents were purchased from Fluka AG (Buchs SG) and used without any further purification. 2-Hydroxyethylamine was freshly distilled before any use. The FT-IR spectra were recorded between 4000–400 cm^{-1} on a JASCO – FT/IR-4200 spectrometer, using the KBr pellet technique at a scanning speed of 16 mm/s with a resolution of 4.0 cm^{-1} . The optical properties of the 2-hydroxyethyl-

amine salts were examined using UV–vis spectrophotometer at room temperature. UV–visible spectrum was recorded in the range of 190–800 nm with PERKIN-ELMER LAMBDA 12 UV–vis spectrometer. Melting points of 2-hydroxyethylammonium salts were found for finely purifying compounds (by repeated recrystallization) using a Boetius instrument and are uncorrected.

Synthesis and Characterization of 1–7 Compounds. The title compounds were prepared by the reaction of 2-hydroxyethylamine and benzoic acid, *p*-methylbenzoic acid, *p*-methoxybenzoic acid, *p*-hydroxybenzoic acid, *p*-chlorobenzoic acid, *p*-bromobenzoic acid and *p*-iodobenzoic acid in a 1:1 molar ratio.¹⁸ Freshly distilled 2-hydroxyethylamine was added in drops to the solution of the acid in an appropriate solvent (diethylether for 1–4, acetone for 5–7) under vigorous stirring at reflux for 2 h to complete the reaction. All the salts formed were precipitated in a white crystalline state and, after cooling at room temperature, were collected by filtration, washed with cold diethylether, respective acetone, and dried in a vacuum for 3 h. This reaction had a yield of about 86–93%. The salts were recrystallized to obtain suitable crystals for the X-ray analysis by slowly cooling their saturated ethanol solutions; the process was accompanied by a slow evaporation of ethanol. The purity of 2-hydroxyethylamine salts was determined via an UV spectrophotometric method, which consisted in determining the acid concentration by measuring the UV absorbance (in NaOH 0.1 M) at λ_{max} of the acid.²⁰ For the seven salts the purity ranged between 97 and 99.5%, with an error of $\pm 0.8\%$.

The elemental analysis was in agreement with the expected stoichiometry. The FT-IR spectra (KBr pellets prepared by grinding a 5–10-mg sample with 100 mg KBr) for each of the six compounds were consistent with salt formation.

The data of chemical/elemental analysis, IR, UV and melting point for compounds 1–7 are provided as Supporting Information.

X-ray Measurements and Refinements. The X-ray data for 1, 3, 5, and 7 were collected at room temperature on Bruker AXS Smart single crystal diffractometer with a CCD detector (MoK_α -radiation); for 2, 4, and 6 on Siemens P3/PC diffractometer (CuK_α -radiation). The crystallographic data and the experimental details are summarized in Table 1. Structure solution and refinement were carried out using the SHELX-97 programs.²¹ Non-hydrogen atoms were refined anisotropically. The empirical absorption correction from the calculated and observed structure factors has been calculated for compounds 5–7.²² Hydrogen atoms were placed in calculated positions with their isotropic displacement parameters riding on those of parent atoms; the H-atoms of NH_3 groups of 2-hydroxyethylamine were found from differential Fourier maps. The geometric parameters for hydrogen bonds are given in Table 3. Selected bond lengths and valence angles for 1–7 are listed in Supporting Information.

Geometric parameters have been calculated and the figures made with the use of the PLATON software.²³ Hydrogen atoms that are not involved in hydrogen bonding were omitted from the representation of crystal packings. Crystallographic data for compounds 1–7 were deposited in the Cambridge Crystallographic Data Center (CCDC 853483, 887607–887609 and 853486–853488, respectively).

RESULTS AND DISCUSSION

The 1:1 stoichiometric reaction of *p*-substituted benzoic acids (1–7) with 2-hydroxyethylamine leads to the formation of stable solid salts in accordance with the appropriate “rule of three”. A distinction between formation of a salt and/or co-crystal and a proper understanding of the process are very important concerning chemical/pharmaceutical development aspects. The pK_a difference (pK_a of base – pK_a of acid) is a tool for predicting salt or co-crystal formation. A larger ΔpK_a (greater than 3) will result in salt formation, and a smaller ΔpK_a (less than 0) will lead to co-crystal formation. But the ΔpK_a value ranging between 0 and 3 was unable to give a clear-cut distinction between co-crystals and salts.²⁵ The differences in pK_a values between the base and acid in all studied

Table 2. Bond Lengths (Å) in Carboxylate Groups and Absolute Values of Their Differences

<i>d</i> (Å)	1	2	3A	3B	4	5	6	7
<i>d</i> 1(C9–O2)	1.244(1)	1.248(4)	1.239(3)	1.268(3)	1.262(3)	1.247(2)	1.245(4)	1.23(1)
<i>d</i> 2(C9–O3)	1.269(1)	1.269(4)	1.271(3)	1.249(3)	1.257(3)	1.271(2)	1.269(4)	1.25(1)
<i>d</i> 1– <i>d</i> 2	0.025	0.021	0.032	0.019	0.005	0.024	0.024	0.02

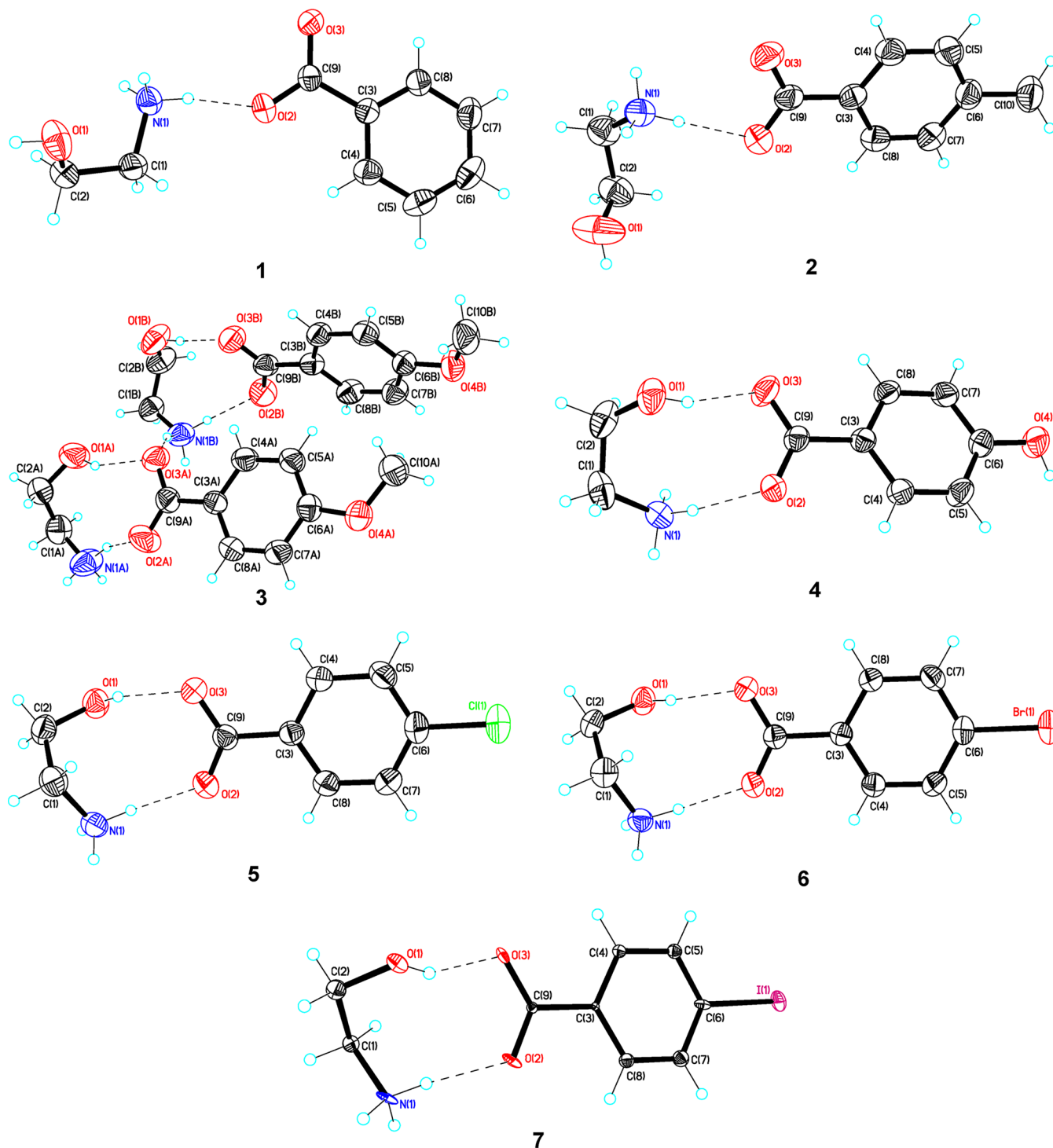


Figure 1. ORTEP drawing for 1–7 with the atomic labeling and charge-assisted hydrogen bonds represented by dashed lines. Thermal ellipsoids are shown with the 50% probability level.

compounds were greater than 3, which determines the extent of proton transfer (Table 3). The studied compounds are water-soluble substances and were obtained in high yields (86–93%)

via an easy one-step synthesis. They have well-defined melting points, generally lower for the salt forms than for the respective benzoic acids; this shows that the neutrality achieved by salt

Table 3. Tabulated ΔpK_a and Hydrogen-Bonding Geometry (\AA , $^\circ$) for Compounds 1–7^a

numbers of HB	ΔpK_a	D–H...A	$d(D\cdots H)$, (\AA)	$d(H\cdots A)$, (\AA)	$d(D\cdots A)$, (\AA)	$\angle(DHA)$, deg	symmetry transformation for H-acceptor
1							
1	5.31	N(1)–H(1)⋯O(2)	0.89	1.81	2.693(1)	170	x, y, z
2		N(1)–H(2)⋯O(3)	0.89	2.15	2.955(1)	150	$-x, -y, -z$
3		N(1)–H(3)⋯O(3)	0.89	2.01	2.884(1)	166	$-x + 1/2, y - 1/2, z$
4		O(1)–H(1)⋯O(3)	0.82	1.96	2.783(1)	176	$x - 1/2, -y - 1/2, -z$
2							
5	5.13	N(1)–H(1)⋯O(2)	0.89	1.98	2.865(3)	173	x, y, z
6		N(1)–H(2)⋯O(3)	0.89	1.90	2.757(3)	163	$-x, -y, z$
7		N(1)–H(3)⋯O(2)	0.89	2.12	2.946(5)	153	$x, -y, z + 1/2$
8		O(1)–H(1)⋯O(2)	0.82	2.01	2.829(3)	176	$-x + 1, -y, z$
3							
9	5.03	N(1A)–H(1)⋯O(3A)	0.89	1.96	2.778(3)	153	$x - 1, y, z$
10		N(1A)–H(2)⋯O(2B)	0.89	1.97	2.850(3)	169	$-x + 1, y + 1/2, -z + 1/2$
11		N(1A)–H(3)⋯O(2A)	0.89	1.89	2.714(3)	154	x, y, z
12		O(1A)–H(1)⋯O(3A)	0.82	1.94	2.691(3)	153	x, y, z
13		N(1B)–H(1)⋯O(3B)	0.89	1.90	2.779(3)	169	$x - 1, y, z$
14		N(1B)–H(2)⋯O(3A)	0.89	2.09	2.937(3)	159	x, y, z
15		N(1B)–H(3)⋯O(2B)	0.89	1.89	2.770(3)	168	x, y, z
16		O(1B)–H(1)⋯O(3B)	0.82	1.90	2.711(3)	169	x, y, z
17		C(10A)–H(1)⋯O(1B)	0.96	2.45	3.355(3)	157	$-x + 5/2, -y + 1, z + 1/2$
18		C(10B)–H(1)⋯O(1A)	0.96	2.41	3.341(3)	163	$-x + 5/2, -y + 1, z + 1/2$
4							
19	4.96	N(1)–H(1)⋯O(2)	0.89	1.91	2.788(2)	167	x, y, z
20		N(1)–H(2)⋯O(2)	0.89	1.86	2.733(2)	167	$x, y + 1, z$
21		N(1)–H(3)⋯O(3)	0.89	2.17	2.878(2)	136	$x, -y + 2, z - 1/2$
22		O(1)–H(1)⋯O(3)	0.82	1.89	2.690(2)	165	x, y, z
23		O(4)–H(1)⋯O(1)	0.82	1.88	2.694(2)	173	$x + 1/2, -y + 1/2, z + 1/2$
24		C(1)–H(1)⋯O(4)	0.97	2.56	3.485(3)	160	$x - 1/2, y + 1/2, z - 1$
25		C(8)–H(1)⋯O(2)	0.93	2.48	3.241(3)	140	$x, -y + 1, z + 1/2$
5							
26	5.52	N(1)–H(1)⋯O(1)	0.89	2.01	2.894(2)	173	$x + 1/2, -y + 1/2, z$
27		N(1)–H(2)⋯O(2)	0.89	1.82	2.701(2)	172	x, y, z
28		N(1)–H(3)⋯O(3)	0.89	1.91	2.793(2)	169	$x + 1, y, z$
29		O(1)–H(1)⋯O(3)	0.82	1.89	2.652(2)	155	x, y, z
30		C(1)–H(1)⋯O(3)	0.97	2.58	3.467(3)	153	$x + 1/2, -y - 1/2, z$
6							
31	5.5	N(1)–H(2)⋯O(1)	0.89	2.01	2.896(4)	175	$x + 1/2, -y + 3/2, z$
32		N(1)–H(1)⋯O(2)	0.89	1.80	2.686(4)	177	x, y, z
33		N(1)–H(3)⋯O(3)	0.89	1.89	2.776(4)	171	$x + 1, y, z$
34		O(1)–H(1)⋯O(3)	0.82	1.84	2.625(4)	161	x, y, z
35		C(1)–H(1)⋯O(3)	0.97	2.54	3.426(5)	152	$x + 1/2, -y + 1/2, z$
7							
36	5.5	N(1)–H(1)⋯O(1)	0.89	2.10	2.91(1)	152	$x + 1/2, -y + 3/2, z$
37		N(1)–H(3)⋯O(2)	0.89	1.87	2.66(1)	146	x, y, z
38		N(1)–H(2)⋯O(3)	0.89	1.99	2.76(1)	143	$x + 1, y, z$
39		O(1)–H(1)⋯O(3)	0.81	1.84	2.59(1)	154	x, y, z
40		C(1)–H(1)⋯O(3)	0.97	2.53	3.41(1)	150	$x + 1/2, -y + 1/2, z$

^aD and A are hydrogen bond donor and acceptor atoms. $\Delta pK_a = pK_a(\text{base}) - pK_a(\text{acid})$ calculating using the pK_a data from SRC PhysProp Database.²⁴ All pK_a values have been determined in aqueous solutions.

forming of zwitterions dramatically decreases the salt melting points.²⁶ The melting-point range for all synthesized salts did not exceed ca. 0.5 °C, which is indicative of their high purity. Elemental analysis indicated 1:1 stoichiometry for all compounds.

Furthermore, the salts were characterized via UV–vis and FT-IR spectroscopy to obtain more information on the chemical structures and the functional groups of those compounds. UV data obtained in NaOH 0.1 M showed that

λ_{max} values are identical for salts and acids; this confirms the existence of the same anion in both compounds.

The UV–Vis spectral studies indicate the cut off wavelength lying between 225.6 and 249 nm for 1–3; 5–7 and 280.3 nm for 4, corresponding to the energy gap of 5.5–5 eV for 1–3; 5–7 and 4.4 eV for 4, which are typical values of insulating materials. The forbidden energy gap was estimated from the values of λ_{max} using the relation $E_g = 1.243 \times 10^3 / \lambda_{\text{max}}$.²⁷ There are no absorption bands in the entire visible region; hence these

Table 4. Computed Dipole Moments (μ , Debye) and Isotropic Dipole Polarizabilities (P, Bohr³) for Anions^a

	1	2	3A	3B	4	5	6
μ_x	-10.7060	-13.4545	-15.0769	-15.4475	-12.4760	-12.1969	-15.0908
μ_y	-0.1008	-0.1289	0.3747	-0.7077	1.2149	-0.1186	-0.1190
μ_z	-0.0269	0.0375	-0.1285	-0.0854	-0.2504	0.0427	-0.0164
μ_{total}	10.6782	13.4147	15.0273	15.4104	11.0607	12.1882	15.1225
P	80.83	91.11	94.23	94.89	101.22	93.49	100.98

^aThe scheme of coordinate system for HF calculations is given in Supporting Information. This system of coordinates where the x axis is perpendicular to the O2...O3 line is common for all studied compounds.

compounds are potential candidates for nonlinear optical applications.

The synthesized salts are IR active species, and their absorption bands occur in different regions. The technique used in the present work brings about plenty of additional information on hydrogen-bonded complexes. Salt formation could be identified by the presence of bands arising from the asymmetric and symmetric vibrations of the COO⁻ group occurring at 1650–1540 cm⁻¹ and 1450–1360 cm⁻¹ and the absence of bands at 1710–1680 cm⁻¹ and 1320–1210 cm⁻¹, characteristic for C=O in a carboxylic group.²⁸ A supplementary proof of the salt formation was the appearance of the C–O stretch belonging to primary alcohols (1100–1000 cm⁻¹, –CH₂OH from ethanolamine), and an additional peak to medium absorption between 2220 and 1820 cm⁻¹ characteristic of primary amine salts.

Crystal Structure Analysis. The salts units of 1–7 serve as building blocks of the supramolecular architecture, and in crystal they are self-assembled *via* ionic N–H...O and normal O–H...O hydrogen bonds (HB) (Figure 1, Table 3).

The identical space groups, in close similarity with chemical structures and lattice parameters of 5–7, suggest some degree of isostructurality between them. The unit cell similarity index is $P = [\{ (a + b + c) / (a_0 + b_0 + c_0) \} - 1]$, where a , b , c and a_0 , b_0 , c_0 are the orthogonalized lattice parameters of the related crystals.²⁹ For similar unit cells $P = 0$, in our case the values of $P_{(56)}$, $P_{(57)}$, $P_{(67)}$ are equal to 0.003, 0.02, and 0.017, respectively. The structures of 5–7 are obviously isostructural, which is evident by the high value of the maximal volumetric isostructurality index,²⁹ which is described as follows: $I_{\text{max}} = [(2 \min\{V_1, V_2\}) / (V_1 + V_2)] \times 100\%$, where V_1 , V_2 are the volumes of the compared fragments. In our case V_1 , V_2 are the molecular volumes of building blocks in asymmetric unit cells. For isostructural pairs (5–6), (5–7), and (6–7), I_{max} are close to 100% and equal to 99.8%, 97.4%, 97.6%, respectively. Therefore, for crystal structures of 5–7 we will further describe only compound 5.

In building blocks of 1 and 2 the cations and anions are held together by one charge-assisted hydrogen bond, while in 3–7 by two (N–H...O and O–H...O) hydrogen bonds. The proton-transferred N–H...O hydrogen bond plays the main role in formation of these pairs and it is present in all investigated salts. The building blocks of 3–7 generate the supramolecular synthons R₂²(9).³⁰ The anions in 1–7 form practically planar systems because the dihedral angles between the least-squares plane of the phenyl ring A (C3C4C5C6C7C8) and the least-squares plane of the COO⁻ groups range from 1.8° to 5.7°. In the asymmetric unit cell of 3, there are two independent building blocks (3A and 3B) where carbon atoms of methyl groups lie practically in the plane of phenyl rings. The torsion angles of C5–C6–O4–C10 range from 1.8° to 3.0°.

The cations in 1–7 adopt the +Syn-Clinal and –Syn-Clinal conformations.²³ The N1C1C2O1 torsion angles in 1, 3A, 5, and in 2, 3B, 4 are equal to 59.8°, 79.2°, 55.1° and –62.0°, –58.2°, –68.8°, respectively. For each of compounds 1 and 2, there are two possibilities to form building blocks using the following charge-assisted hydrogen bonds with N...O separations: 2.693 (1), (1A), 2.884(1) (1B), 2.865 (3) (2A) and 2.757(3) (2B) Å (Table 3). For this reason, the total HF³¹ energies have been calculated for these systems in order to choose the optimal building blocks: –627.2256 (1A), –627.2196 (1B), –666.2585 (2A), –666.22324 (2B) a.u. Thus, the 1A and 2A BB were selected to study the supramolecular architecture of compounds 1–7. The cation was the same for all studied compounds; therefore, the analysis of both dipole moments (DM) and isotropic polarizabilities³¹ of anions was carried out so as to understand why in 1 and 2 anions and cations are held together by one proton-transferred hydrogen bond while in 3–7 by two hydrogen bonds (Table 4).

The increase of the dipole moment in 2, when hydrogen in 1 is replaced by the methyl group, can be referred to the inductive effect, which leads to the development of charges. But the value of DM in 2 is greater than in 4 and 5, which may be due to the substituent effect. The hydroxyl group is an electron-withdrawing one inductively but it is an electron-donating group through resonance. Halogen substituents are a little unusual and they are both inductive electron withdrawing (electronegativity) and resonance donating (lone pair donation). For example, the charges of Cl and Br atoms in 5 and 6 are equal to 0.109 and –0.010, respectively. However, the dipole polarizabilities in 3–6 are greater than in 1, 2, which leads to increasing the instantaneous dipoles formation in 3–6 because the polarizability refers to the ability of the electron distribution in a molecule to change temporarily. The fluctuating dipole corresponds to the permanent dipole; therefore, the polar molecules interact both through their permanent dipoles and through the correlated, instantaneous fluctuations in those dipoles. The polarizability affects dispersion forces which play a significant role in the formation of two N–H...O and O–H...O hydrogen bonds between the cations and anions in 3–7. The two above-mentioned hydrogen bonds are also observed when an H atom in *para*-position is substituted by an electron withdrawing NO₂⁻ group.⁶ Thus in the studied molecular aggregates the substituent effect influences both the dipole–dipole interactions and the dispersion interactions between anions and cations, which leads to intermolecular force fields driving the organization of one charge-assisted (1, 2) hydrogen bond or two (3–7) hydrogen bonds in building blocks. The complexation energies of single molecular building blocks ΔE_1 show a better complexation efficiency for the proton-transfer complexes of 3A, 3B and 4 than for 1 and 2 (Table 5), while the values of

Table 5. Computed Total SCF Energies (E , au) and Energy Differences for 1–6^a

	1	2	3A	3B	4	5	6
E_1	−627.2256	−666.2585	−741.0897	−741.1035	−702.0901	−1086.1522	−3196.5822
E_{anion}	−417.6843	−456.7011	−531.5491	−531.5483	−492.5430	−876.6099	−2987.0414
E_{cation}	−209.3798	−209.3768	−209.3563	−209.3644	−209.3628	−209.3671	−209.3627
ΔE_1	−0.1615	−0.1806	−0.1843	−0.1908	−0.1843	−0.1752	−0.1781
ΔE_2	−0.1911	−0.20241		−0.2015	−0.193	−0.1836	−0.1904
ΔE_3	−0.0355	−0.0436		−0.028	−0.0175	−0.0168	−0.0245

^a E_1 denotes the SCF energy of single molecular building block.

Table 6. Shortest Intermolecular Contacts (d) between Pairs of Building Blocks and Computed Total SCF Energies (E , au) and Energy Differences for 1–6

	1A	1B	1C	2A	2B	2C	3A	3B
d (Å)	2.884	2.783	2.955	2.757	2.946	2.829	2.778	2.779
E_{tot}	−1254.4804	−1254.4819	−1254.4979	−1332.5762	−1332.5548	−1332.5509	−1482.2116	−1482.2347
E_2	−627.2402	−627.241	−627.249	−666.2881	−666.2774	−666.2755	−741.1058	−741.1174
ΔE_2	−0.1761	−0.1769	−0.1849	−0.2102	−0.1995	−0.1976	−0.2004	−0.2047
ΔE_3	−0.0292	−0.0307	−0.0467	−0.0592	−0.0378	−0.0339	−0.0322	−0.0277
	3AB	3BA	4A	4B	5A	5B	6A	6B
d (Å)	2.850	2.937	2.878	2.694	2.793	2.894	2.776	2.896
E_{tot}	−1482.236	−1482.2024	−1404.2094	−1404.1859	−2172.3339	−2172.3084	−6393.2016	−6393.1762
E_2	−741.1178	−741.1012	−702.1047	−702.0921	−1086.167	−1086.1542	−3196.6008	−3196.5881
ΔE_2	−0.2087	−0.1921	−0.1989	−0.1872	−0.1899	−0.1967	−0.1967	−0.184
ΔE_3	−0.0428	−0.0092	−0.0292	−0.0057	−0.0295	−0.0372	−0.0372	−0.0118

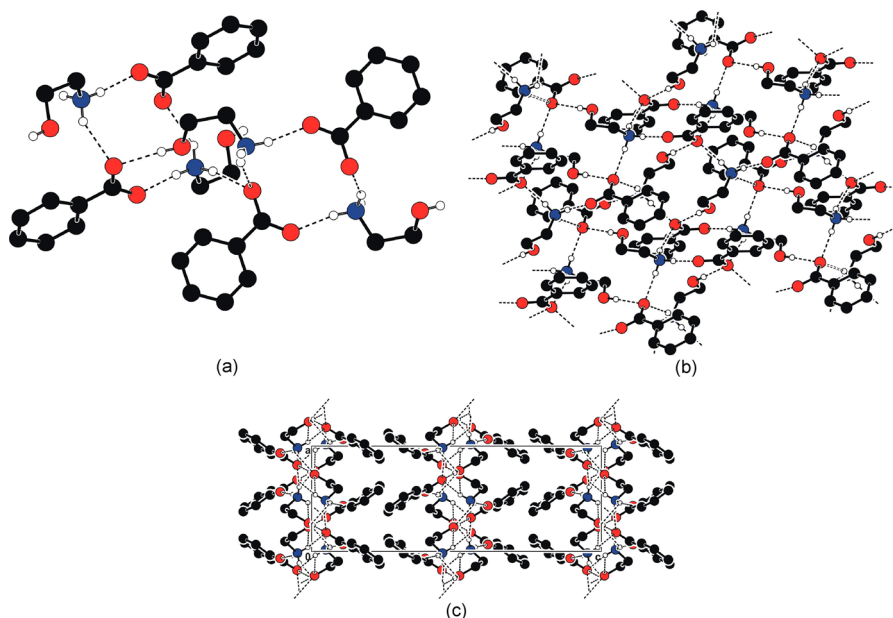


Figure 2. (a) Fragment of the layer showing synthons formation and main hydrogen bonds in Table 2. (b) Crystal packing of 1 representing the 2-D layers parallel to (001) plane. (c) Fragment of molecular packing in the crystal of 1.

ΔE_1 for 5 and 6 are comparable with that in 2. In order to estimate how the environment (i.e., the neighboring building blocks in the studied crystal structures) influenced the complexation energies ΔE_1 , the calculations of the following quantities were performed (Table 6): (a) the total SCF energies (E_{tot}) for nearest pairs of building blocks in 1–6; (b) the total energies (E_2) of a single building block belonging to the given pair of nearest building blocks. The shortest intermolecular contacts for non-hydrogen atoms (d) between each pair of building blocks in the investigated compounds, as well as the energies for complexation of neighboring building

blocks (ΔE_3) in the pairs and for the given building blocks (ΔE_2) are presented in Table 6. The averaged values of ΔE_2 and ΔE_3 are summarized in Table 5. The presence of neighboring building blocks in the studied crystal structures has led to a higher complexation efficiency for the salts units of 1–6 which are building blocks of the supramolecular architecture (Table 5). From the point of view of crystal growth and design, it is important to analyze the energies for complexation of building blocks in 1–6. The complexation energies ΔE_3 (Tables 5 and 6) show better complexation efficiency for 1 and 2 in comparison with that in complexes 3–

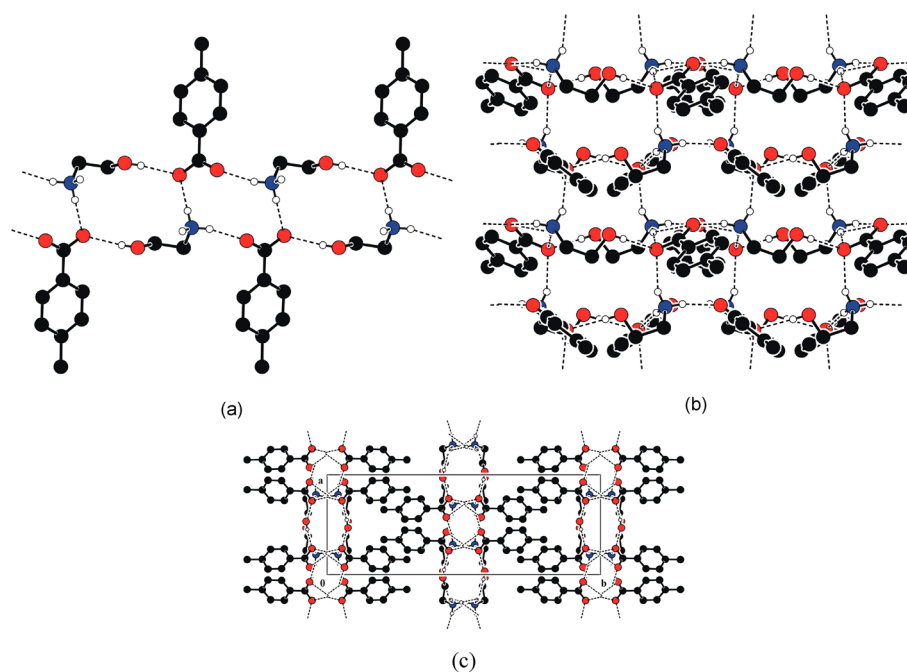


Figure 3. (a) The chains along the *a* direction where the synthons are related by N(1)⋯O3 (6) hydrogen bonds. (b) View of layer formation where chains are joined by N(1)⋯O2 (7) hydrogen bonds. (c) Fragment of molecular packing in the crystal of 2.

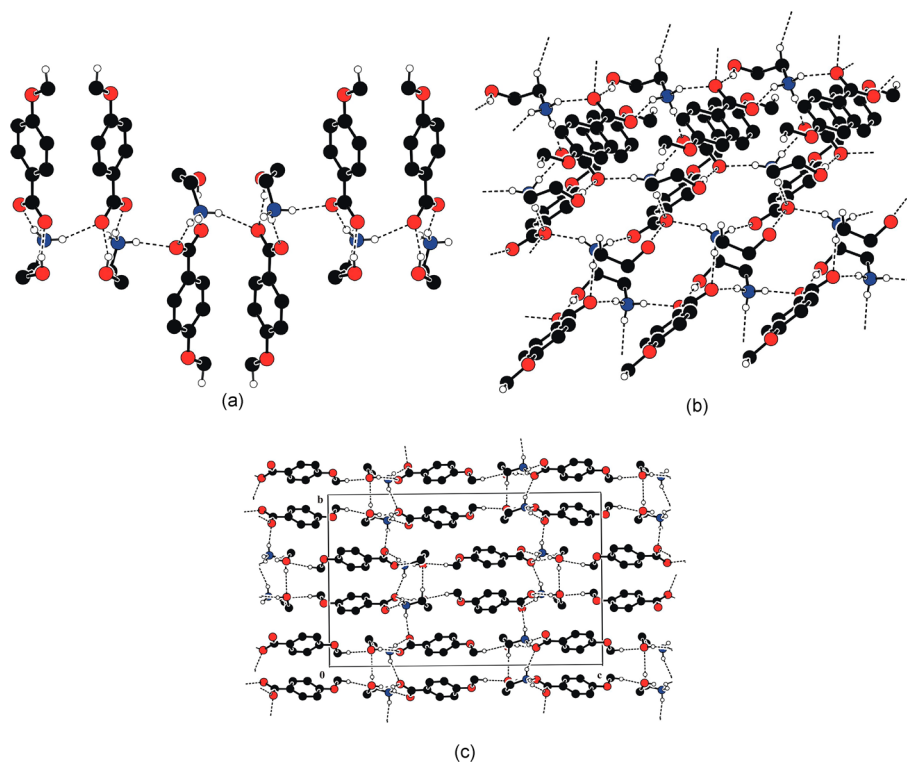


Figure 4. (a) Chains along the *b* direction in 3 where building blocks are linked by N1A⋯O2B (10) and N1B⋯O3A (14) hydrogen bonds. (b) View of layer formation where translation related along the *a* axis chains are joined by N1A⋯O3A (9) and N1B⋯O3B (13) HB. (c) The crystal packing of 3 showing interactions between layers *via* C(10A)⋯O(1B) (17) and C(10B)⋯O(1A) (18) hydrogen bonds.

6 because in the BB of 1 and 2 the cations and anions are held together by one charge-assisted hydrogen bond N–H⋯O while in 3–6 by two hydrogen bonds. It means that in 1 and 2 the O–H⋯O hydrogen bond is involved in linking with the neighboring building blocks, whereas in 3–6 the given hydrogen bond participates in formation of building blocks.

In 1, $R_4^2(12)$ antidromic intermolecular rings around a symmetry center are formed by building blocks *via* N1⋯O2 (1) and N1⋯O3 (2) hydrogen bonds. These synthons are further related by a glide planes perpendicular to $[1\ 0\ 0]$ with the glide component $[0\ 0.5\ 0]$ and 2-fold screw axes with direction $[100]$ and screw component $[0.5\ 0\ 0]$ due to N1⋯O3 (3) and

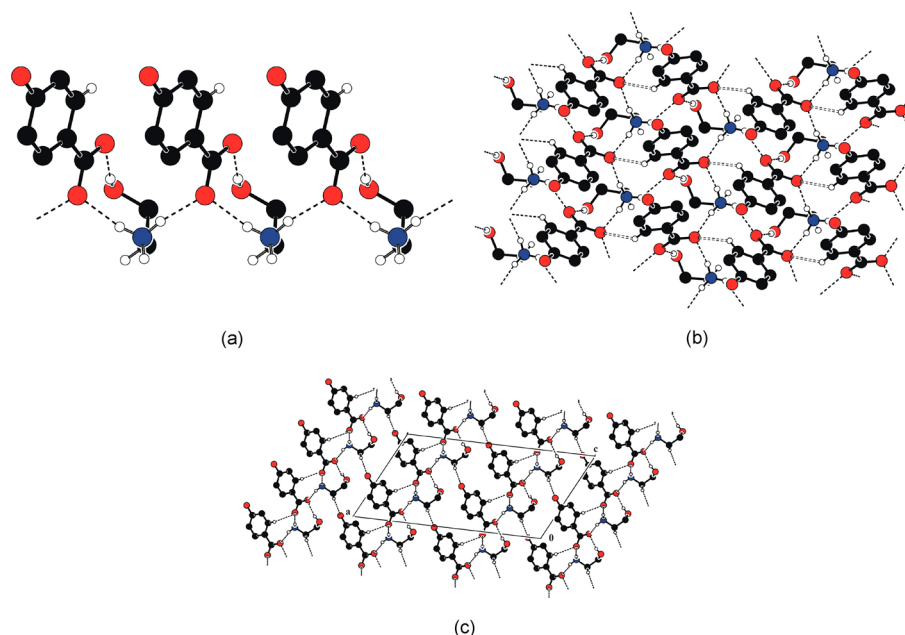


Figure 5. (a) View of the H-bonded chain running along the *b* direction due to translation. Building blocks form chains *via* N1...O2 (20) hydrogen bonds. (b) These chains are joined by glide planes through the N1...O3 (21) and C8...O2 (25) hydrogen bonds and assemble into 2-D layers. (c) Fragment of molecular packing in **4** showing interactions between layers O4...O1 (23) and C1...O4 (24) hydrogen bonds.

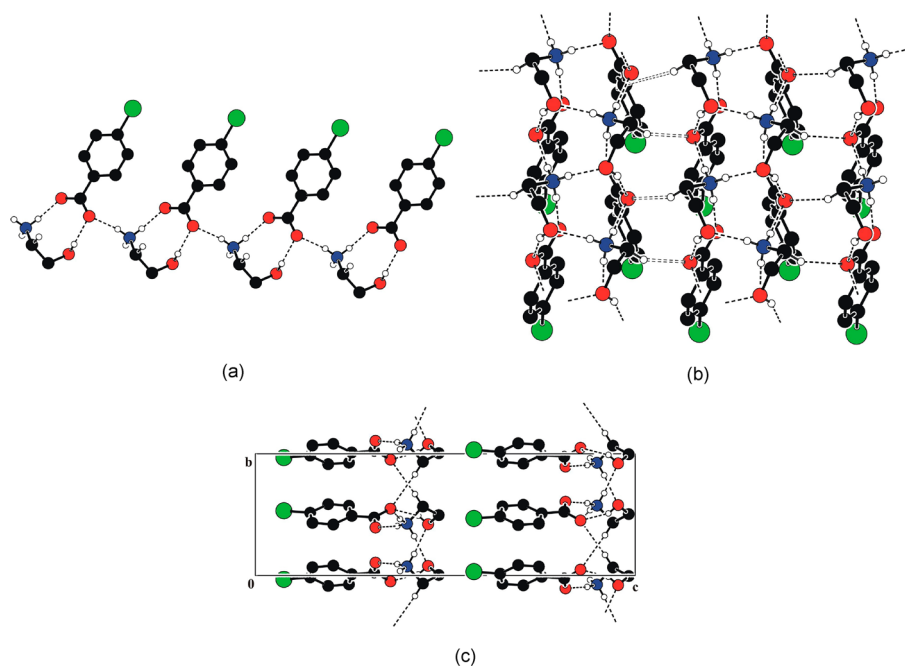


Figure 6. (a) Fragment of the chain in **5**. BB form the chains due to translation along the *a* direction *via* N1...O3 (28) hydrogen bonds. (b) These chains are joined by glide planes through N1...O1 (26) and C1...O3 (30) hydrogen bonds forming the layers. (c) Fragment of molecular packing in the crystal of **5**.

O1...O3 (4) HB and assemble into 2-D layers parallel to the (001) plane (Figure 2a,b, Table 3). According to the criterion proposed by others:²³ the distance of Cg(J1)...Cg(J2) < 6.0 Å, $\beta < 60.0^\circ$, where β is the angle between the Cg(J1)Cg(J2) vector and the normal to the J1 ring, there are the π - π stacking interactions between the phenyl rings Cg(A) and Cg(A) ($1/2 + x, y, 1/2 - z$), laying in different layers of **1** (Figure 2c). The Cg(J1)...Cg(J2) distance between the centroids of these moieties is 4.81 Å and $\beta = 9.5^\circ$. In **1** there is a X-H...Cg (π -ring) interaction (H...Cg < 3.0 Å, $\gamma < 30.0^\circ$, where γ is the

angle between the HCg vector and the normal to the aromatic ring).²³ For the C1-H...Cg(A) ($-1/2 + x, y, 1/2 - z$) interaction, the distance between the H atom and A centroid is 2.94 Å, while the angle γ is 14.41° . The C1-H bonds and phenyl rings lie in different layers. The X-H...Cg interaction is observed within the layers for C5-H bonds, where H...Cg(A) ($1 + x, y, z$) distances and γ values are equal to 2.89 Å and 13.69° , respectively.

In **2**, the $R_2^2(14)$ antidromic intermolecular rings around the 2-fold rotation axes are formed by building blocks *via* N1...O2

(5) and O1...O2 (8) hydrogen bonds. These synthons are further related by a translation due to N(1)...O3 (6) HB and assemble into chains developed along the *a* direction in the unit cell. The chains are further consolidated into 2-D layers parallel to the (010) plane through the N(1)...O2 (7) hydrogen bonds *via* the glide planes which are perpendicular to *a* axis with glide component [0 0 0.5] (Figure 3a,b, Table 3). There are the π - π stacking interactions between the phenyl rings Cg(A) and Cg(A) ($-x, y, -1/2 + z$), laying in different layers of **2** (Figure 3c).

The Cg(J1)...Cg(J2) distance between the centroids of these moieties is 5.03 Å and $\beta = 12.0^\circ$.

In the crystal structure of **3**, the building blocks form the helix-like chains along *b* direction due to 2-fold screw axis *via* N1A...O2B (10) and N1B...O3A (14) hydrogen bond (Figure 4a, Table 3). Translations related along *a* axis chains are further consolidated into 2-D layers parallel to (001) plane through N1A...O3A (9) and N1B...O3B (13) hydrogen bonds (Figure 4b). The layers in **3** are linked by C(10A)...O(1B) (17) and C(10B)...O(1A) (18) hydrogen bonds (Figure 4c).

In **3** there are both π - π stacking interactions between the phenyl rings Cg(A(C3AC4AC5AC6AC7AC8A)) and Cg(B(C3BC4BC5BC6BC7BC8B)) and X-H...Cg(A,B) interactions within the layers. The Cg(A)...Cg(B) ($1 - x, -1/2 + y, 1/2 - z$) and Cg(B)...Cg(A) ($-x, 1/2 + y, 1/2 - z$) distances between the centroids of these moieties are equal to 4.922 and 4.875 Å, and the values of β angles are equal to 14.71 and 14.92°. The H...Cg(A) ($1 - x, 1/2 + x, 1/2 - z$) and H...Cg(B) ($-x, 1/2 + x, 1/2 - z$) separations and γ angles for distances C5B-H and C5A-H are equal to 2.90, 2.92 Å and 7.8, 12.9°, respectively.

The building blocks of **4** form the chains due to translation along the *b* direction *via* N1...O2 (20) HB. These chains are further related by a glide plane perpendicular to [0 1 0] with the glide component [0 0 0.5] through the N1...O3 (21) and C8...O2 (25) HB and assemble into 2-D layers parallel to (100) plane (Figure 5a,b, Table 3). The layers in **4** are linked by O4...O1 (23) and C1...O4 (24) hydrogen bonds (Figure 5c) due to the glide plane perpendicular to [0 1 0] with the glide component [0.5 0 0.5] and the centering vector [0.5 0.5 0].

In the crystal structure of **5** the building blocks form the chains along the *a* direction due to translation *via* N1...O3 (28) hydrogen bond (Figure 6a, Table 3). The chains are further consolidated into 2-D layers through N1...O1 (26) and C1...O3 (30) hydrogen bonds. These layers propagate parallel to the (001) plane where the chains are related by glide planes perpendicular to [0 1 0] with the glide component [0 0 0.5] (Figure 6b).

Within the layers in **5** there are short phenyl rings Cg(A)...Cg(A) ($-1/2 + x, 1/2 - y, z$) as well as X-H...Cg(A) ($-1/2 + x, 1/2 - y, z$) interactions. The distance between the centroids of cycles is equal to 4.738 Å and $\beta = 14.5^\circ$. The H...Cg(A) separation and γ angles for distance C5-H are 2.81 Å and 8.2°, respectively. There are van der Waals interactions between the layers with short Cl...O1($2 - x, 1 - y, 1/2 + z$) contacts which are equal to 3.263(2) Å (Figure 6c).

There is an effect of hydrogen bonding on the geometry of carboxylate groups. While all carboxylate groups in **1-7** participate as hydrogen-bonding acceptors, the C-O bond lengths vary significantly with the number and type of hydrogen-bonding donors linked to the oxygen atom. In the absence of hydrogen bonding and other electronic perturbations, the C-O bond lengths should be equal because of

electron delocalization.⁶ Formation of single or multiple hydrogen bonds at one oxygen atom should cause the associated C-O bond to lengthen. Thus the differences in C-O bond lengths in carboxylate groups vary between 0.005 and 0.032 Å in **1-7** that is more than three times their esd's (Table 2), with the exception of compounds **4** and **7**.

As expected from the non-centrosymmetric space groups for crystal structures of **2-7**, they may exhibit second-harmonic generation that is related to nonlinear optical applications. For the studied compounds, the calculations of macroscopic polarizations (*P*) of unit cell using the SIESTA method³² show a sizable value of *P* mainly directed along the direction of the *c* axis for **3, 5-7** and the *a* axis for **4** (Table 7).

Table 7. Macroscopic Polarization Per Unit Cell (*P*, Debye) along Lattice Vectors

CN	<i>P_a</i>	<i>P_b</i>	<i>P_c</i>
2	14772.898521	140319.877225	12895.569495
3	10047.748369	24175.314416	38077.850088
4	18638.082667	3371.104062	8656.148086
5	4517.534205	5535.750654	15703.515070
6	4572.795134	5603.466959	13704.447941
7	4517.534205	5508.859092	17177.652181

For all these structures, macroscopic polarizations are practically perpendicular to layers formed by building blocks *via* hydrogen bonds. For **2**, where the building blocks are self-assembled by one hydrogen bond, the orientation of *P* is not related to crystal packing.

CONCLUSIONS

2-Hydroxyethylammonium salts of *para*-substituted benzoic acids were synthesized and characterized by X-ray diffraction analysis. Their structures display a number of certain common structural features. In the crystal packing, the building blocks of **1-7** are self-assembled *via* proton-transferred N-H...O and normal O-H...O hydrogen bonds. In the building blocks of **1** and **2**, the cations and anions are held together by one charge-assisted hydrogen bond N-H...O while in **3-7** by two hydrogen bonds. In the studied compounds, the substituent effect influences dipole-dipole interactions as well as the dispersion interaction between anions and cations, which leads to intermolecular force fields driving the organization of one charge-assisted (**1, 2**) hydrogen bond or two (**3-7**) hydrogen bonds in building blocks. The complexation energies ΔE_1 of single molecular building blocks show a better complexation efficiency for the proton-transfer complexes of **3A, 3B** and **4** than for **1** and **2**, while the values of ΔE_1 for **5** and **6** are comparable with that in **2**. However, the environment of building blocks in the studied crystal structures has influenced the complexation energies ΔE_1 . The presence of neighboring building blocks in crystal structures has led to a higher complexation efficiency for the salts units of **1-7** which are building blocks of the supramolecular architecture. The crystal growth of the studied compounds depends on the energies for complexation of neighboring building blocks (ΔE_3). The values ΔE_3 show a better complexation efficiency for **1** and **2** in comparison with complexes **3-6**, because in the building blocks of **1** and **2** the cations and anions are held together by one charge-assisted hydrogen bond N-H...O while in **3-6** by two hydrogen bonds. It means that in **1** and **2** the O-H...O hydrogen bond is involved in linking the neighboring building

blocks, whereas in 3–6 the given hydrogen bond participates in the formation of building blocks. In all studied compounds, the BB are consolidated into 2-D layers through the N–H...O and O–H...O hydrogen bonds. There is an effect of hydrogen bonding on the geometry of carboxylate groups in 1–7. While all carboxylate groups in 1–7 participate as hydrogen-bonding acceptors, the C–O bond lengths vary significantly with the number and type of hydrogen-bonding donors linked to the oxygen atom. As expected from the non-centrosymmetric space groups for crystal structures of 2–7, they may exhibit the second-harmonic generation, which is related to nonlinear optical applications. For structures, where the building blocks are self-assembled by two hydrogen bonds, the macroscopic polarizations are practically perpendicular to layers formed by building blocks *via* hydrogen bonds. The structures reported here further demonstrate the utility of the 2-hydroxyethylamine cation to be incorporated into synthons so as to generate stable hydrogen-bonded structures.

■ ASSOCIATED CONTENT

● Supporting Information

The X-ray crystallographic information files (CIF) are available for compounds 1–7. Data on chemical analyses (elemental analysis, IR, UV and melting point), selected bond lengths and angles and computational details are provided free of charge *via* the Internet at <http://pubs.acs.org/>.

■ AUTHOR INFORMATION

Corresponding Author

*E-mail: xray52@mail.ru; telephone: +37322738154; fax +37322738149.

Notes

The authors declare no competing financial interest.

■ ACKNOWLEDGMENTS

This work was financially supported by Project 2.2 of the Institute of Chemistry Timisoara of Romanian Academy. The authors thank Dr. Gabriele Bocelli for X-ray data collection.

■ REFERENCES

- (1) (a) Bis, J. A.; Zaworotko, M. J. *Cryst. Growth Des.* **2005**, *5*, 1169–1179. (b) Sarma, B. N.; Balakrishna, K. N.; Bhogala, N.; Nangia, A. *Cryst. Growth Des.* **2009**, *9*, 1546–1557. (c) MacGillivray, L. R. *CrystEngComm* **2002**, *4*, 37–41. (d) Olenik, B.; Smolka, T.; Boese, R.; Sustmann, R. *Cryst. Growth Des.* **2003**, *3*, 183–188. (e) Aakeroy, C. B.; Desper, J.; Urbina, J. F. *Cryst. Growth Des.* **2005**, *5*, 865–873. (f) Saha, B. K.; Nangia, A.; Jaskolski, M. *CrystEngComm* **2005**, *7*, 355–358. (g) Shattock, T. R.; Vishweshwar, P.; Wang, Z.; Zaworotko, M. J. *Cryst. Growth Des.* **2005**, *5*, 2046–2049. (h) Aakeroy, C. B.; Salmon, D. J. *CrystEngComm* **2005**, *7*, 439–448. (i) Morissette, S. L.; Almarsson, O.; Peterson, M. L.; Remenar, J. F.; Read, M. J.; Lemmo, A. V.; Ellis, S.; Cima, M. J.; Gardner, C. R. *Adv. Drug Delivery Rev.* **2004**, *56*, 275–300.
- (2) (a) Thomas, R.; Kulkarni, G. U. *J. Mol. Struct.* **2008**, *873*, 160–167. (b) Lemmerer, A.; Bernstein, J.; Kahlenberg, V. *J. Chem. Crystallogr.* **2011**, *41*, 991–997. (c) Aakeröy, C. B.; Seddon, K. R. *Chem. Soc. Rev.* **1993**, *22*, 397–407. (d) Jeffery, G. A. *Introduction to Hydrogen Bonding*; Wiley: Chichester, 1997. (e) Jeffery, G. A.; Saenger, W. *Hydrogen Bonding in Biology and Chemistry*; Springer-Verlag: Berlin, 1993.
- (3) (a) Kodama, K.; Sekine, E.; Hirose, T. *Chem.—Eur. J.* **2011**, *17*, 11527–11534. (b) Zhang, X.-L.; Chen, X.-M. *Cryst. Growth Des.* **2005**, *5*, 617–622. (c) Ranganathan, A.; Pedireddi, V. R.; Rao, C. N. R. *J. Am. Chem. Soc.* **1999**, *121*, 1752–1753. (d) Swift, J. A.; Pivovar, A. M.; Reynolds, A. M.; Ward, M. D. *J. Am. Chem. Soc.* **1998**, *120*, 5887–5894. (e) Taylor, R.; Kennard, O. *J. Am. Chem. Soc.* **1982**, *104*, 5063–5070. (f) Pedireddi, V. R.; Prakasha, R. J. *Tetrahedron Lett.* **2002**, *43*, 4927–4930.
- (4) (a) Felix, O.; Hosseini, M. W.; De Cian, A.; Fischer, J. *J. Chem. Soc., Chem. Commun.* **2000**, *2000*, 281–282. (b) Felix, O.; Hosseini, M. W.; De Cian, A.; Fischer, J. *Angew. Chem., Int. Ed. Engl.* **1997**, *36*, 102–104. (c) Ballabh, A.; Trivedi, D. R.; Dastidar, P.; Suresh, E. *CrystEngComm* **2002**, *4*, 135–142. (d) Trivedi, D. R.; Ballabh, A.; Dastidar, P. *CrystEngComm* **2003**, *5*, 358–367. (e) Ballabh, A.; Trivedi, D. R.; Dastidar, P. *Cryst. Growth Des.* **2005**, *5*, 1545–1553.
- (5) (a) Aakeröy, C. B.; Nieuwenhuysen, M. *J. Am. Chem. Soc.* **1994**, *116*, 10983–10991. (b) Aakeröy, C. B. *Acta Crystallogr.* **1997**, *B53*, 569–586.
- (6) Chumakov, Yu. M.; Simonov, Yu. A.; Grozav, M.; Crisan, M.; Bocelli, G.; Yakovenko, A. A.; Lyubetsky, D. *Central Eur. J. Chem.* **2006**, *4*, 458–475.
- (7) (a) Bhogala, B. R.; Nangia, A. *Cryst. Growth Des.* **2003**, *3*, 547–554. (b) Jeffrey, G. A. *An Introduction to Hydrogen Bonding*; Oxford University Press: Oxford, 1997.
- (8) (a) Smith-Becker, J.; Marois, E.; Huguet, E. J.; Midland, S. L.; Sims, J. J.; Keen, N. T. *Plant Physiol.* **1998**, *116*, 231–238. (b) Senaratna, T.; Merritt, D.; Dixon, K.; Bunn, E.; Touchell, D.; Sivasithamparam, K. *Plant Growth Regulat.* **2003**, *39*, 77–81. (c) Cueva, C.; Moreno-Arribas, M. V.; Martín-Alvarez, P. J.; Bills, G.; Vicente, M. F.; Basilio, A.; Rivas, C. L.; Requena, T.; Rodríguez, J. M.; Bartolome, B. *Res. Microbiol.* **2010**, *161*, 372–382.
- (9) Nagalakshmi, R.; Krishnakumar, V.; Hagemann, H.; Muthunatesan, S. *J. Mol. Struct.* **2011**, *988*, 17–23.
- (10) Chen, Z.; Peng, M. *J. Chem. Crystallogr.* **2011**, *41*, 137–142.
- (11) (a) McDonald, J. C.; Dorrestein, P. C.; Pilley, M. M. *Cryst. Growth Des.* **2001**, *1*, 29–35. (b) Zhao, P. S.; Wang, X.; Jian, F. F.; Zhang, J. L.; Xiao, H. L. *J. Serb. Chem. Soc.* **2010**, *75*, 459–473. (c) Tan, T. *J. Mol. Struct.* **2007**, *840*, 6–13.
- (12) Parshad, H.; Frydenvang, K.; Liljefors, T.; Sorensen, H. O.; Larsen, C. *Int. J. Pharm.* **2002**, *237*, 193–207.
- (13) Ishida, H.; Rahman, B.; Kashino, S. *Acta Crystallogr., Sect. C* **2001**, *57*, 1450–1453.
- (14) (a) Smith, G.; Wermuth, U. D.; Bott, R. C.; White, J. M.; Willis, A. C. *Aust. J. Chem.* **2001**, *54*, 165–170. (b) Gotoh, K.; Katagiri, K.; Ishida, H. *Acta Crystallogr., Sect. E* **2010**, *66*, 3190.
- (15) Wang, Y.; Luo, Y. H.; Feng, W.; Che, Y. X.; Zheng, J. M. *Chin. J. Struct. Chem.* **2006**, *25*, 449–452.
- (16) Bruno, I. J.; Cole, J. C.; Edgington, P. R.; Kessler, M. K.; Macrae, C. F.; McCabe, P.; Pearson, J.; Taylor, R. *Acta Crystallogr., Sect. B: Struct. Sci.* **2002**, *58*, 389–397.
- (17) Allen, F. H. *Acta Crystallogr., Sect. B: Struct. Sci.* **2002**, *58*, 380–388.
- (18) Crisan, M.; Grozav, M.; Kurunczi, L.; Ilia, G.; Berteau, C. *J. Plant Interact.* **2007**, *2*, 53–61.
- (19) Crisan, M.; Grozav, M.; Berteau, C. *J. Plant Interact.* **2009**, *4*, 271–277.
- (20) Dorosencu, M.; Rad, R.; Grozav, M.; Neamtii, I. *Ann. West Univ. Timisoara* **2001**, *10*, 337–342.
- (21) Sheldrick, G. M. *SHELX-97. Program for the Solution and Refinement of Crystal Structure*; University of Gottingen: Gottingen, Germany, 1997.
- (22) Parkin, S.; Moezzi, B.; Hope, H. *J. Appl. Crystallogr.* **1995**, *28*, 53–56.
- (23) Spek, A. L. *J. Appl. Crystallogr.* **2003**, *36*, 7–13.
- (24) SRC PhysProp Database: <http://www.syrres.com/what-we-do/databaseforms.aspx?id=386>
- (25) (a) Bhogala, B. R.; Basavoju, S.; Nangia, A. *CrystEngComm* **2005**, *7*, 551–562. (b) Childs, S. L.; Stahly, G. P.; Park, A. *Mol. Pharmaceutics* **2007**, *4*, 323–338. (c) Mohamed, S.; Tocher, D. A.; Vickers, M.; Karamertzanis, P. G.; Price, S. L. *Cryst. Growth Des.* **2009**, *9*, 2881–2889. (d) Hathwar, V. R.; Pal, R.; Row, T. N. G. *Cryst. Growth Des.* **2010**, *10*, 3306–3310.

- (26) Mazzenga, G. C.; Berner, B. J. *Controlled Release* **1991**, *16*, 77–88.
- (27) Khandpekar, M. M.; Pati, S. P. *Opt. Commun.* **2010**, *283*, 2700–2704.
- (28) Silverstein, R. M.; Webster, F. X. *Spectrometric Identification of Organic Compounds*, 6th ed.; John Wiley & Sons: New York, 1998.
- (29) Fabian, L.; Kalman, A. *Acta Crystallogr. B.* **1999**, *55*, 1099–1108.
- (30) Grell, J.; Bernstein, J.; Tinhofer, G. *Acta Crystallogr., Sect. B* **2000**, *56*, 166.
- (31) Frisch, M. J.; Trucks, G. W.; Schlegel, H. B.; Scuseria, G. E.; Robb, M. A.; Cheeseman, J. R.; Montgomery, J. A.; Vreven, T.; Kudin, K. N.; Burant, J. C.; Millam, J. M.; Iyengar, S. S.; Tomasi, J.; Barone, V.; Mennucci, B.; Cossi, M.; Scalmani, G.; Rega, N.; Petersson, G. A.; Nakatsuji, H.; Hada, M.; Ehara, M.; Toyota, K.; Fukuda, R.; Hasegawa, J.; Ishida, M.; Nakajima, T.; Honda, Y.; Kitao, O.; Nakai, H.; Klene, M.; Li, X.; Knox, J. E.; Hratchian, H. P.; Cross, J. B.; Adamo, C.; Jaramillo, J.; Gomperts, R.; Stratmann, R. E.; Yazyev, O.; Austin, A. J.; Cammi, R.; Pomelli, C.; Ochterski, J. W.; Ayala, P. Y.; Morokuma, K.; Voth, G. A.; Salvador, P.; Dannenberg, J. J.; Zakrzewski, V. G.; Dapprich, S.; Daniels, A. D.; Strain, M. C.; Farkas, O.; Malick, D. K.; Rabuck, D.; Raghavachari, K.; Foresman, J. B.; Ortiz, J. V.; Cui, Q.; Baboul, A. G.; Clifford, S.; Cioslowski, J.; Stefanov, B. B.; Liu, G.; Liashenko, A.; Piskorz, P.; Komaromi, I.; Martin, R. L.; Fox, D. J.; Keith, T.; Al-Laham, M. A.; Peng, C. Y.; Nanayakkara, A.; Challacombe, M.; Gill, P. M. W.; Johnson, B.; Chen, W.; Wong, M. W.; Gonzalez, C.; Pople, J. A. *GAUSSIAN 03*, Revision B.01: Gaussian, Inc.: Pittsburgh, PA, 2003.
- (32) Soler, J. M.; Artacho, E.; Gale, J. D.; Garcia, A.; Junquera, J.; Ordejon, P.; Sanchez-Portal, D. *J. Phys.: Condens. Matter.* **2002**, *14*, 2745–2779.